ИНСТИТУТ ЯДЕРНОЙ ФИЗИКИ СО АН СССР

S.E. Baru, A.G. Khabakhpashev, L.I. Shekhtman

MULTIWIRE PROPORTIONAL CHAMBER FOR DIGITAL RADIOGRAPHIC INSTALLATION

PREPRINT 89-39

НОВОСИБИРСК

Multiwire Proportional Chamber for Digital Radiographic Installation

S.E. Baru, A.G. Khabakhpashev, L.I. Shekhtman

Institute of Nuclear Physics
630090, Novosibirsk 90, USSR

ABSTRACT

A fast one-coordinate multiwire proportional chamber for digital radiography is described. To obtain high spatial resolution in every part of the chamber together with high counting rate capability and quantum efficiency the anode wires are stretched along radial directions with center at the focus of the *X*-ray tube of radiographic installation. The cathode planes are inclined relative to the anode plane to effect uniform gas amplification along an anode wire. The main characteristics of the chamber are: spatial resolution 1.2 mm, quantum efficiency 28% (∼60 keV), counting rate capability 600 kHz/channel

INTRODUCTION

Described in [1] was a digital radiographic installation for medical diagnostics, permitting to reduce exposure doses by 30—100 times and to obtain an *X*-ray image in digital form, well known for its merits. In order to obtain an image the slit collimator forms a narrow flat beam which penetrates through a patient's body and gets into the inlet window of the multiwire proportional chamber (Fig. 1). The chamber measures an *X*-ray distribution along a horizontal direction, a distribution along another coordinate is measured by a mechanical scanning. For this purpose standard *X*-ray tube, the collimator and the chamber was moved simultaneously in vertical direction. The multiwire proportional chamber (MWPC) worked like 160 practically independent *X*-ray quanta counters. Each anode wire through an amplifire-discriminator was connected to a scaler. A digital image was stored in a computer memory.

The main defect of the first version of the installation was limited spatial resolution of the MWPC. A detector for digital radiography must have counting rate capability of 70—100 MHz. When using MWPC such a counting rate can be achieved only with parallel readout of information from anode wires, and to reduce space charge effects working length of the anode wires must be about several centimeters. It demands the anode wires to be directed to the source of radiation. Spatial resolution of such a chamber depends on the step of the anode wires. In the chamber [1] the step

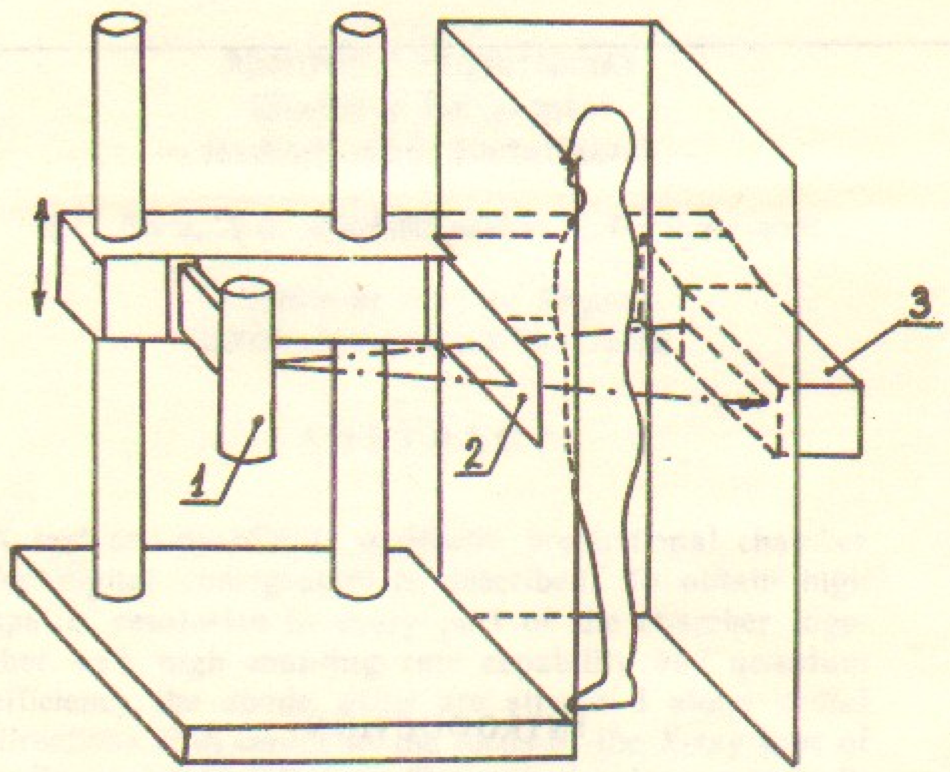

Fig. 1. Digital radiographic installation.

was 2 mm. Since the anode wires as in all proportional chambers was parallel to each other, spatial resolution was worse at the edges of the chamber due to parallax. In such a chamber design a reduction of the step between the wires allows to improve the resolution only in the centre of the chamber. At the edges of the chamber parallax, connected to finite distance between the focus of the tube and the chamber (1300 mm) will remain the resolution practically constant. That's why there was made the chamber which had the anode wires stretched along radial directions with centre at the focus of the X-ray tube and the step of ~1 mm. The number of channels was increased to 256.

THE CHAMBER WITH FAN ANODE PLANE

The chamber with such anode plane permits to solve the problem of improving spatial resolution of the digital radiographic installation. However, the gas gain of a proportional chamber depends on a distance between anode wires. Therefore in order to exclude changes of the gain along the anode wires and thus to avoid making amplitude resolution and counting rate capability worse, the cathode planes must be inclined at a definite angle relative to anode plane. As follows from [2] gas gain M depends on a

distance between anode wires S and a gap anode—cathode l only through a capacity of anode wire C, that is

$$M = G[C(S, l)], \tag{1}$$

and so the condition of the gain to be constant along an anode wire can be obtained

$$dM = \frac{\partial M}{\partial C}\left(\frac{\partial C}{\partial l}dl + \frac{\partial C}{\partial S}dS\right) = 0. \tag{2}$$

The capacity of an anode wire is

$$C = \frac{2\pi\varepsilon_0}{\frac{\pi l}{S} - \ln\left(\frac{2\pi a}{S}\right)}, \tag{3}$$

where a—radius of an anode wire. From (2) and (3) we can obtain:

$$\frac{dl}{l} = \frac{dS}{S} - \frac{dS}{\pi l}. \tag{4}$$

In our case $l = 2$ mm, $S = 1.2$ mm and with a mistake about 10% one can account

$$\frac{dl}{l} = \frac{dS}{S}. \tag{4'}$$

The design of the chamber for the digital radiographic installation is shown at Fig. 2. As in [1] the chamber is placed in duralumin box so that an X-ray beam gets into the gap between the drift electrode and the upper cathode. The length of the anode wires is 50 mm, diameter is 10 μm. The distance between the focus of the X-ray tube and the centre of the chamber is 1300 mm, the step of anode wires at the inlet window side is 1200 μm, at the opposite side 1246 μm. Anode—cathode gap is about 2 mm, cathode planes inclined to 77 μm (calculated from (4')).

To measure the dependence of the gain on a coordinate along an anode wire the chamber was put into a special unit with lavsan window in its cover. Radioactive source (Cd^{109}) and a slit collimator of 2·40 mm were placed above the window. The measured dependence is shown at Fig. 3. At the 40 mm region from $x = 5$ mm to $x = 45$ mm relative changes of gain do not exceed 10%.

In order to estimate a change of gas amplification along an

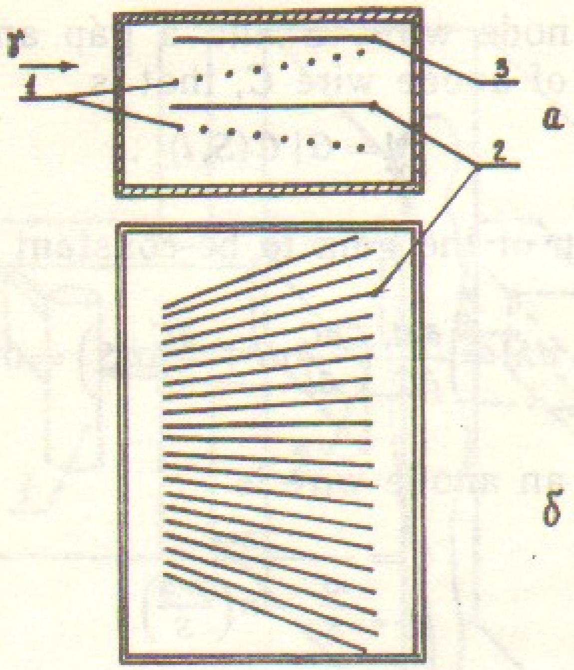

Fig. 2. Multiwire proportional chamber: *a* — side view; *b* — top view of anode plane: *1* — cathode planes; *2* — anode plane; *3* — drift electrode.

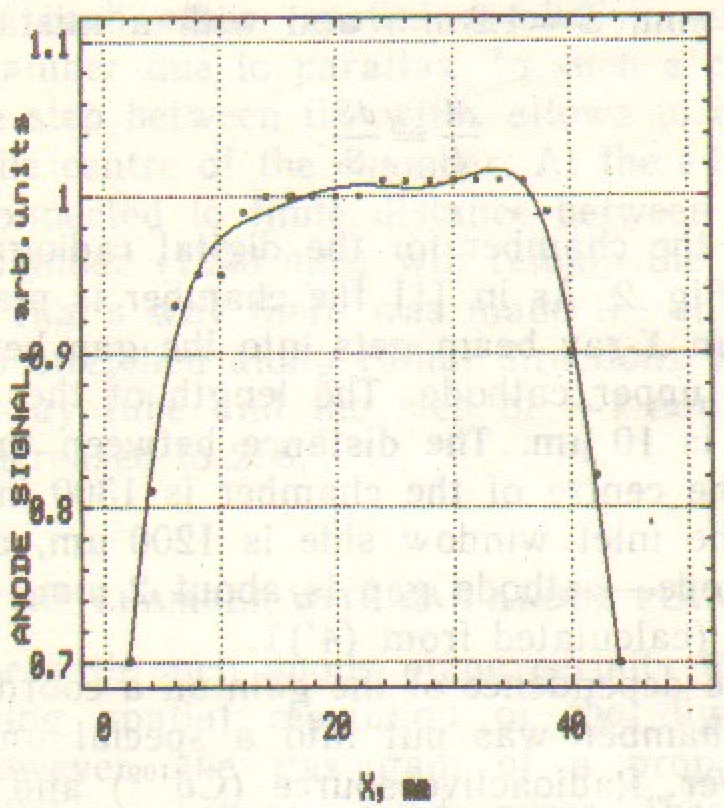

Fig. 3. Dependence of anode signal on coordinate along anode wire.

anode wire with fan anode and parallel cathode planes there was made a special chamber of diminished size. The measurements performed on this chamber showed that at 40 mm working length of an anode wire the change of gain equals 27%. Thus inclined cathode planes permit to compensate gain change appearing due to fan anode plane.

SPATIAL RESOLUTION

During an *X*-ray quantum absorbtion by a Xe atom several number of secondary particles are produced, that are: photoelectrons, Auger-electrons and fluorescent photons. Ranges of these particles affect the spatial resolution of the chamber causing in some cases a simultaneous operation of several channels.

An absorbtion of *X*-ray quantum with the energy exceeding Xe *K*-shell (34.6 keV) proceeds mainly in two ways — on the *K*-shell (~80%) and on the *L*-shell (~20%). During the *K*-shell absorbtion except a photoelectron with the energy of (E_γ — 34.6 keV) there can be emitted a fluorescent photon (29.5 ÷ 34.6 keV) or Auger-electron ~24 keV. *L*-shell interaction causes ejecting of photoelectron with the energy of (E_γ — 5.4 keV). If the energy of *X*-ray quantum equals 60 keV photo- and Auger-electrons have a range in Xe at 3 atm about 1 mm and can cause simultaneous operation of two neighbouring channels, and photoelectrons emitted after *L*-shell interaction can cause even 3 channel operation. The absorbtion process is considered more carefully in [3]. In this paper also the algorithms for simulation the described processes are discussed. Usage of this algorithms taking into account the geometry of our

Table

The Probabilities of Channel Counting While Incident Quantum is Absorbed in Channel Number 0 (Simulation)

N Channel	h_i, %
1	11.2
2	1.6
3	0.46
4	0.34
5	0.23

chamber permits to calculate probabilities h_i of simultaneous counting of channel number i while absorbing quantum in channel 0 (Table). The calculation was made for radiation of X-ray tube with tungsten anode at a 70 kV voltage, copper filter of 0.3 mm and a pressure of working mixture ($Xe+20\%CO_2$) 3 atm.

Results, presented in Table, shows that a probability of counting of two neighbouring channels is much more than one of channels which are at a distance from each other. Hence the main distortions connected to double registration of X-ray quanta will be caused by coincidences of neighbouring channels. For their excluding there were used a corresponding selecting circuit.

A coincidence of neighbouring channels occurs mainly when photo- or Auger-electron crosses a boundary between them. For such events formed, as a rule, close to the boundary between channels, primary ionization is divided into two parts. Therefore the exception of such coincidences improve both spatial and amplitude resolution. An essential shortcoming of the method of coincidence suppression is reduction of system efficiency by about 30% for X-rays with average energy of 50—60 keV.

Spatial resolution of detectors with channel structure (an example of such a detector is MWPC with described method of

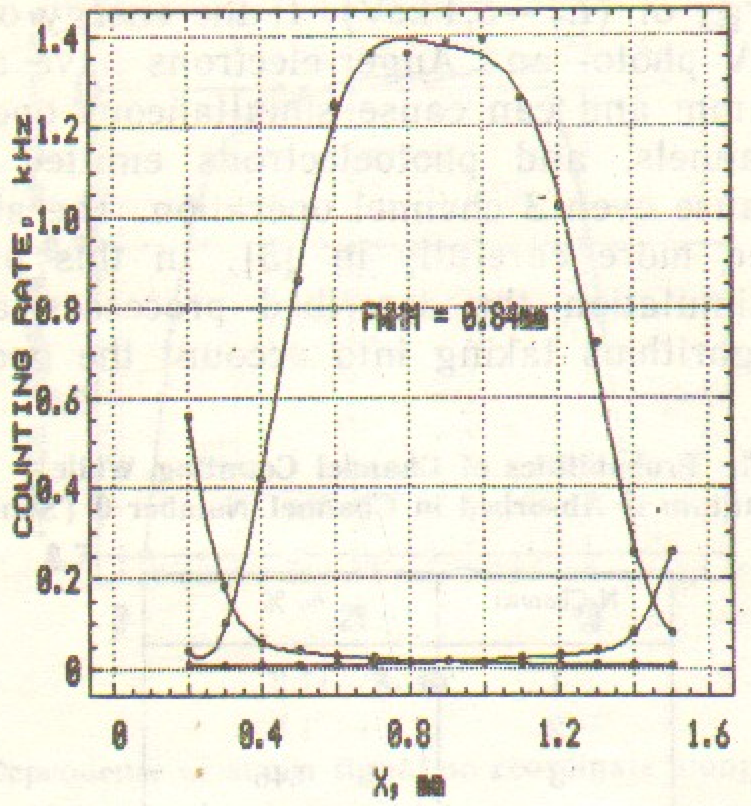

Fig. 4. Shape of a channel of the MWPC. To the right and to the left from the main curve begin the curves for neighbouring channels.

readout) is described completely by a channel shape function, that is the dependence of a channel counting rate on a position of narrow collimated source of radiation. At Fig. 4 the curve of channel shape is shown, obtained by irradiating the chamber with an X-ray beam from a tube with 70 kV voltage and 0.3 mm copper filter (effective energy 47 keV). FWHM is 0.84 mm. This value is less than the anode wires step — 1.2 mm, because exception of coincidences results mainly in excluding of events registrated besides channel boundaries.

However, for many practical purposes it is more convenient to describe spatial resolution by one parameter with the help of contrast-frequency responce function (CFR) — by a spatial frequency at a definite contrast level. The method to define CFR is described in (3). To measure it one should take a set of grids with periods of λ_i made from opaque for X-rays material. At an image of such a grid the dependence of counting rate on the number of a row (or a colomn, if a vertical resolution is measured) is periodical. The CFR is defined as

$$C(\nu) = \frac{N_{max} - N_{min}}{N_{max}}, \qquad (5)$$

where $\nu = 1/\lambda$ — a spatial frequency, N_{min} — average value of all channels with counting rate less than average counting rate $\bar{N}$; N_{max} — average value of the channels which have $N_i > \bar{N}$.

The CFR defined in such a way describes spatial resolution well in those cases when a detector channel size δ is much less than a grid period. In our case these values are comparable and, for example, when using a grid with $\lambda = 2\delta$ the value of C depends on phase position between boundaries of a grid and a channel. In order to exclude this ambiguity it is necessary to make averaging over the phase. For this purpose all grids were chosen so that $\lambda/2\delta$ differed from natural values and from multiples of 0.5. At such a condition an image of a grid has «beats», that is the amplitude of oscillations is changed periodically depending on a shift of the phase between boundaries of a grid and a channel. In this case for calculation the value of C it's enough to perform averaging over a period of «beats».

The results of measurements of CFR at the centre and the sides of the chamber when irradiating by X-rays from a tube with a 70 kV voltage are presented at Fig. 5. If one defined spatial resolution as a frequency at $C = 0.5$ it can be noticed that there is no

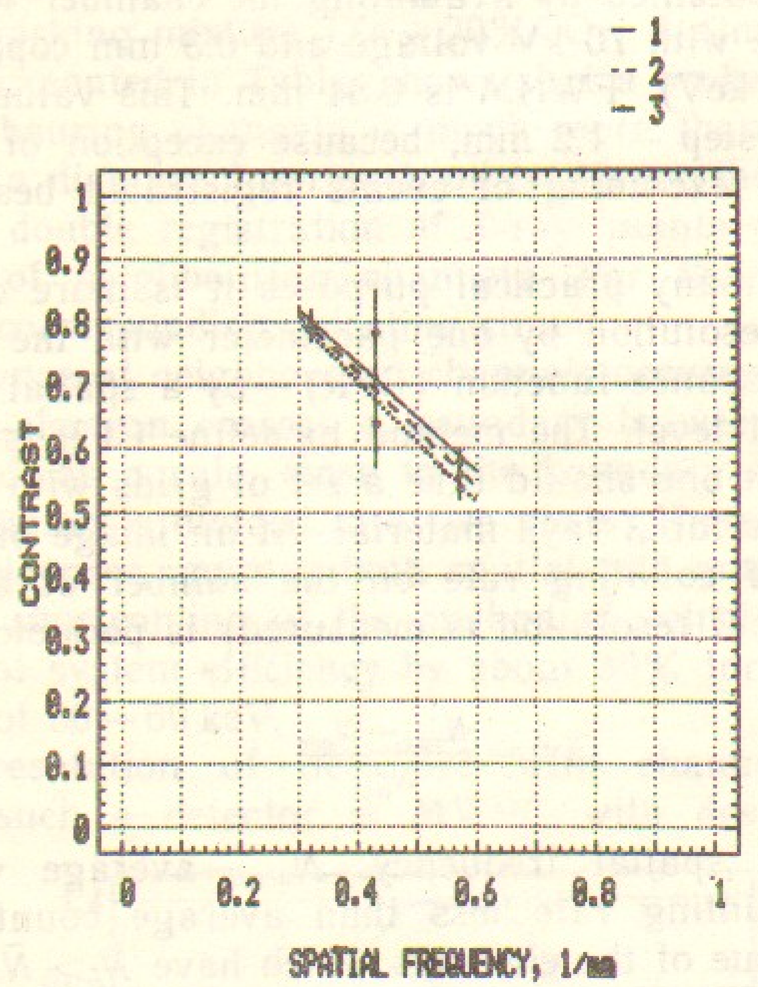

Fig. 5. Contrast-frequency response functions:
1—at the centre of MWPC; *2*—at the left side (channel number ~20); *3*—at the right side (channel number ~240). Accuracy of measurements at $\nu = 0.46$ is worse than at other values, because the period of corresponding grid is about a doubled size of the MWPC channel. This makes the beats, appearing at the image of grid, to have large period, which cause significant errors during calculation of *C*.

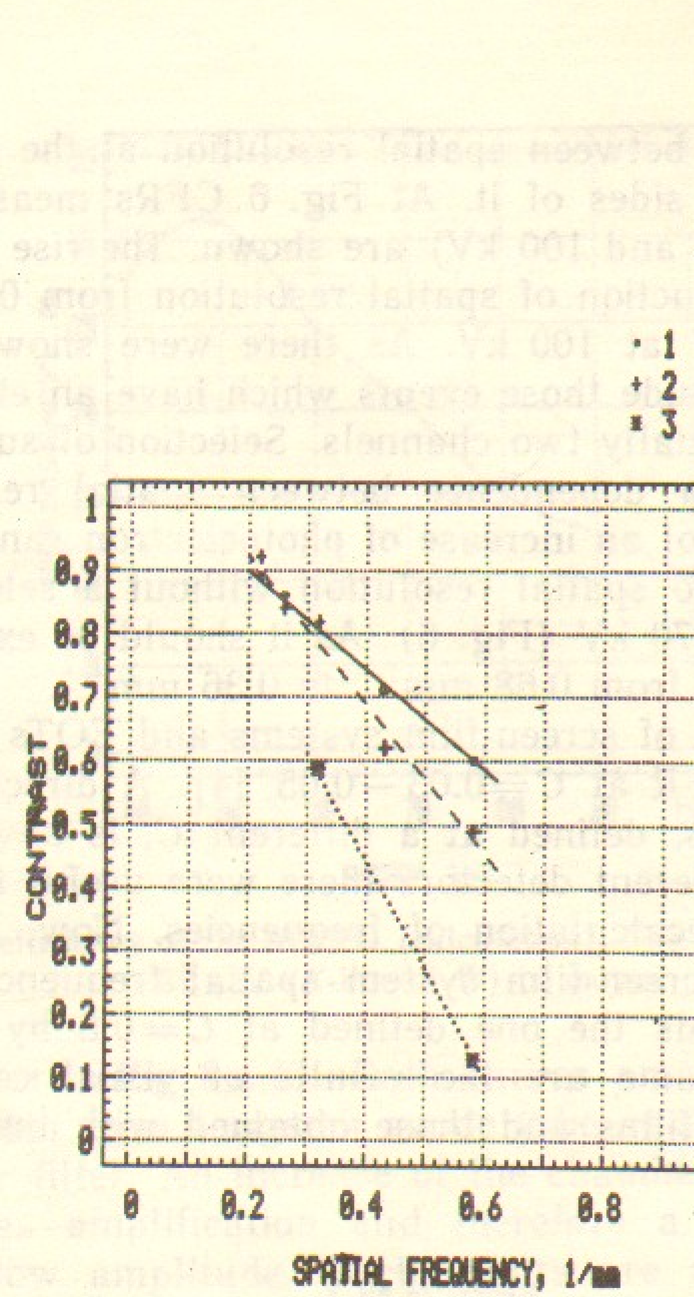

Fig. 6. CFR functions measured at different tube voltages and at a different conditions of event selection:
1—tube voltage 70 kV; *2*—tube voltage 100 kV; *3*—selection circuit switched off.

essential differencies between spatial resolution at the centre of the chamber and at the sides of it. At Fig. 6 CFRs measured at two tube voltages (70 kV and 100 kV) are shown. The rise of an *X*-rays energy results in reduction of spatial resolution from 0.68 mm^{-1} at 70 kV to 0.56 mm^{-1} at 100 kV. As there were shown above the selecting circuits exclude those events which have an electron range crossing at least partially two channels. Selection of such an events reduces essentially a dependence between spatial resolution and *X*-ray energy inspite of an increase of photoelectron range.

We measured also spatial resolution without a selection circuit at a tube voltage of 70 kV (Fig. 6). As it should be expected spatial resolution reduced from 0.68 mm^{1-} to 0.36 mm^{-1}.

Spatial resolution of screen-film systems and EOTs is defined in radiography from CFR at $C=0.03-0.05$ [4]. A direct comparison of spatial frequencies, defined at a different *C*, is obviously incorrect. To compare different detectors there were useful to find quantitative method of recalculation of frequencies. Now, we can only point out that for screen-film system spatial frequency defined at $C=0.03\div0.05$ exceeds the one defined at $C=0.5$ by 2—3 times. Approximately the same are the results of visual comparison of images obtained on films and those obtained with the help of the MWPC.

EFFICIENCY

A calculated dependence of the MWPC efficiency on radiation energy is presented at Fig. 7. To perform the calculation there were taken into account a thickness of the Al inlet window — 1 mm; a layer of working mixture which absorbs *X*-rays without detection — 27 mm; efficient length of anode wires — 45 mm. The calculation is made for a working mixture $Xe+20\%CO_2$ at 3 atm pressure. Presented at this figure is also the result of measurement of the efficiency at the energy of 57 keV (W^{181}). There was measured a full counting rate of *X*-ray quanta (the selecting circuit was switched off, simultaneous counting of two and more channels were considered as one event). A CsI(Na) crystal with photomultiplyer was used for monitoring. Measured efficiency of 28% well agrees with calculation.

To choose a working voltage at the chamber and at the drift electrode there were measured the dependence of counting rate on

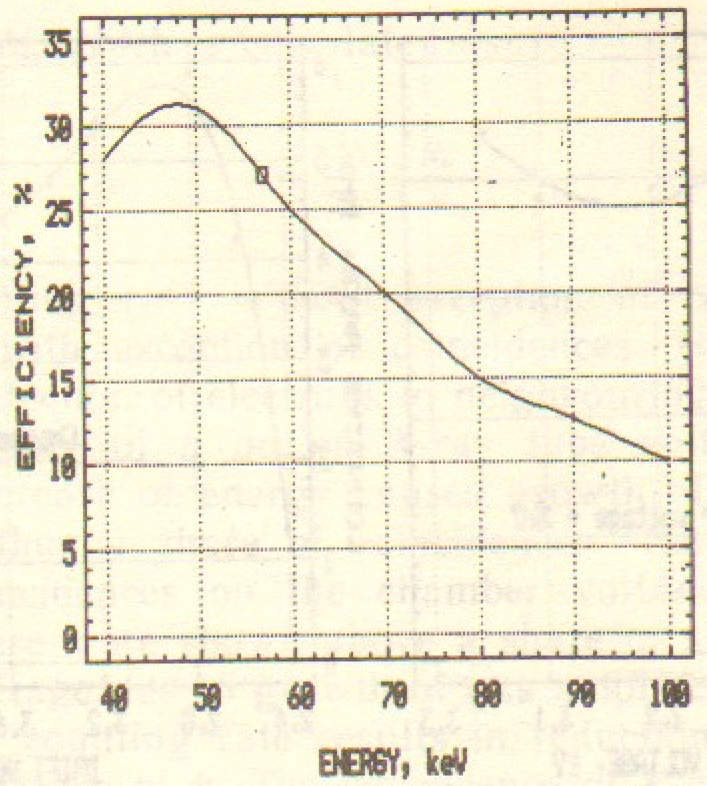

Fig. 7. Quantum efficiency of the MWPC (calculation). The result of measurement at 57 keV (*K*-line of W) is shown.

these parameters (Fig. 8,*a*,*b*). Both curves are obtained by irradiating the chamber by a tungsten anode tube at a 70 kV voltage with 0.3 mm copper filter. An increase of the chamber voltage causes the growth of gas amplification and therefore a part of registrated events with low amplitude. Such events are mainly connected to coincidences of neighbouring channels which are excluded by a selection circuit. This fact explains a reduction of the efficiency at the plateau when increasing the voltage at the cathode and at the drift electrode.

A working voltage at the chamber is chosen at the centre of the plateau. To choose a voltage at the drift electrode there were measured the dependence of event amplitude on this voltage 8,*c*. The working point is chosen so to provide a complete charge collection from the drift gap. The chosen voltage at the chamber is 2.8 kV, at the drift electrode is 4.8 kV.

An exception of coincidence of neighbouring channels results in dependence of a complete efficiency of the detector on both the efficiency of detection of *X*-rays by the chamber and a part of events which cause coincidences of neighbouring channels. There was measured a dependence of a number of coincidences on different factors. To characterize a number of coincidences there were taken a

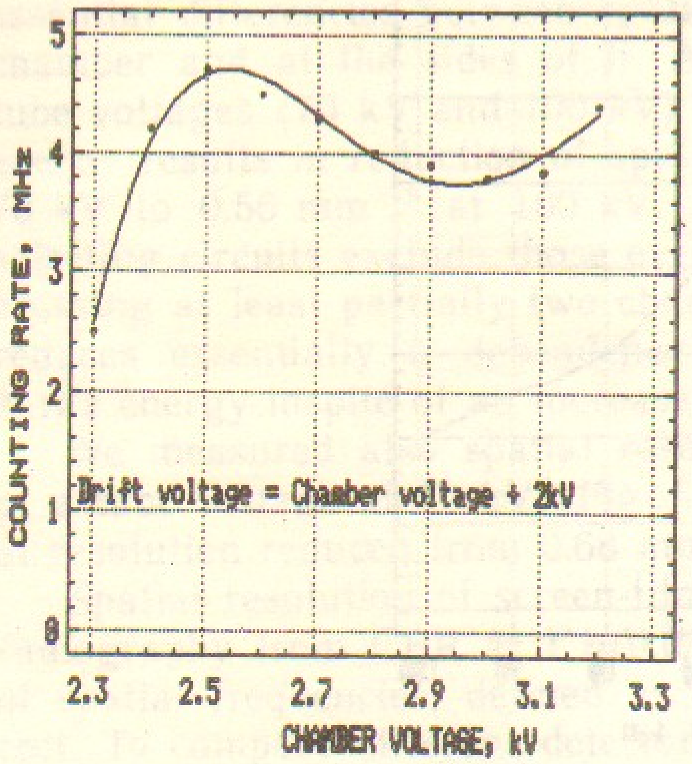

a

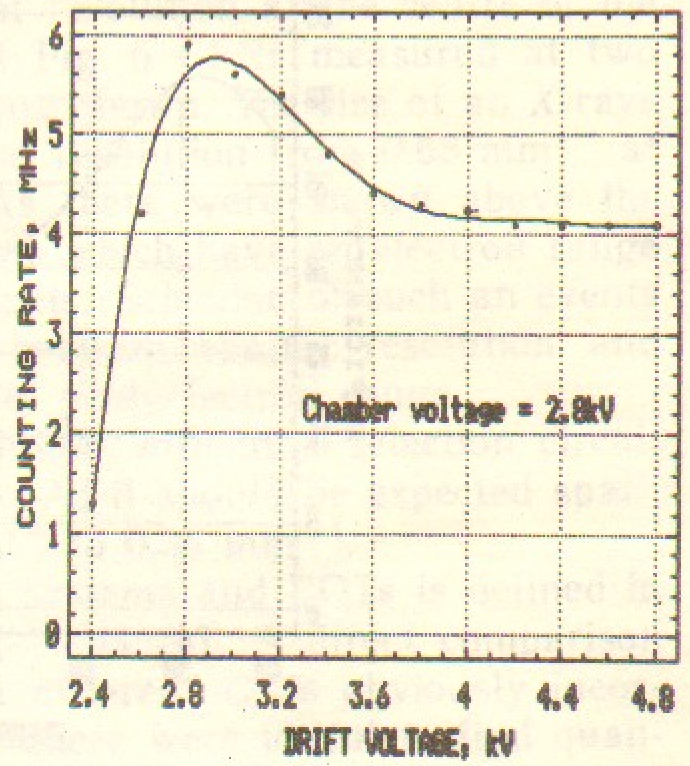

b

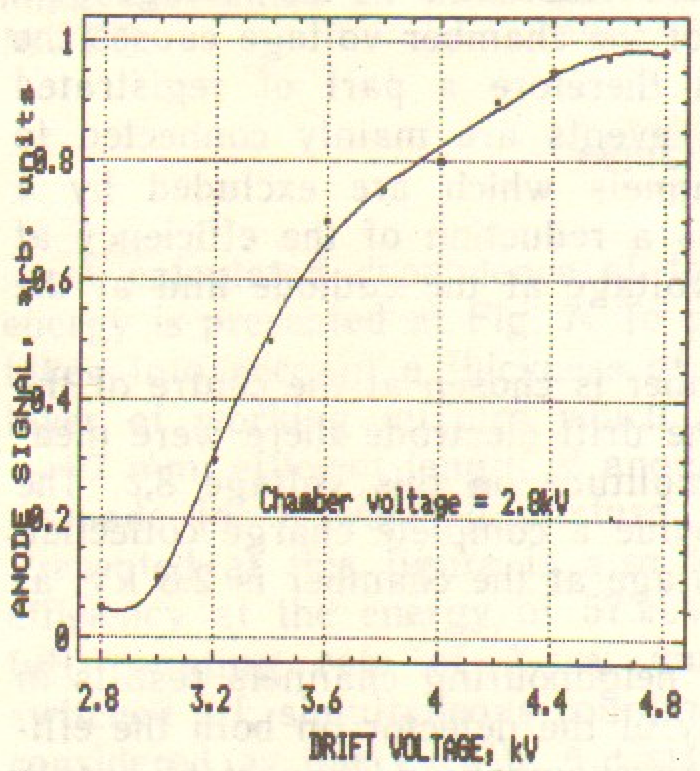

c

Fig. 8.
a — Dependence of count rate on cathode voltage of MWPC; *b* — dependence of count rate on drift electrode voltage; *c* — dependence of anode signal on voltage of the drift electrode.

value of $h = \sum_i h_i'$, which is calculated as

$$h = \frac{N - N_0}{2(N + N_0)}, \qquad (6)$$

where N — counting rate without exception of coincidences, N_0 — counting rate with exception of coincidences. Here h_i' takes into account only detection of electrons in neighbouring channels.

The dependence of h on an *X*-ray tube voltage is shown at Fig. 9,*a*. An increase of energy causes growth of ranges of photo-electrons and thus a share of coincidences. The dependence of a number of coincidences on the chamber voltage is presented at Fig. 9,*b*. As there were shown above a share of such events increases with the voltage due to growth of gas amplification. An increase of the chamber counting rate results in reduction of gas gain and therefore in decrease of h. The dependence of h on a counting rate is shown at Fig. 9,*c*.

The measurements show that a share of coincidences can be changed significantly due to different conditions of the chamber operation. However the measured value of h does not exceed 21%. This value of h is reached at a minimal counting rate and tube voltage of 100 kV.

COUNTING RATE CAPABILITY

A counting rate capability of the MWPC depends on space charge accumulated in a working volume at high rates [5, 6], and dead time of the electronics.

Errors of the electronics depends on a dead time of the amplifiers — discriminators and a dead time of selection circuit. The dead time of discriminators leads to reduction of the efficiency of a single events detection with an increase of counting rate. The dead time of a selection circuit results in registration of a part of coincidences as a single events and, therefore, to a partial compensation of the errors, connected to a dead time of discriminators. A dead time of amplifiers — discriminators in our case is approximately equal to a dead time of selection circuit. At such a condition a counting rate after the selection circuit makes up.

$$N_0 = n_0(1 - 3n\tau + 0.5n_c\tau) + 0.25n_c n\tau, \qquad (7)$$

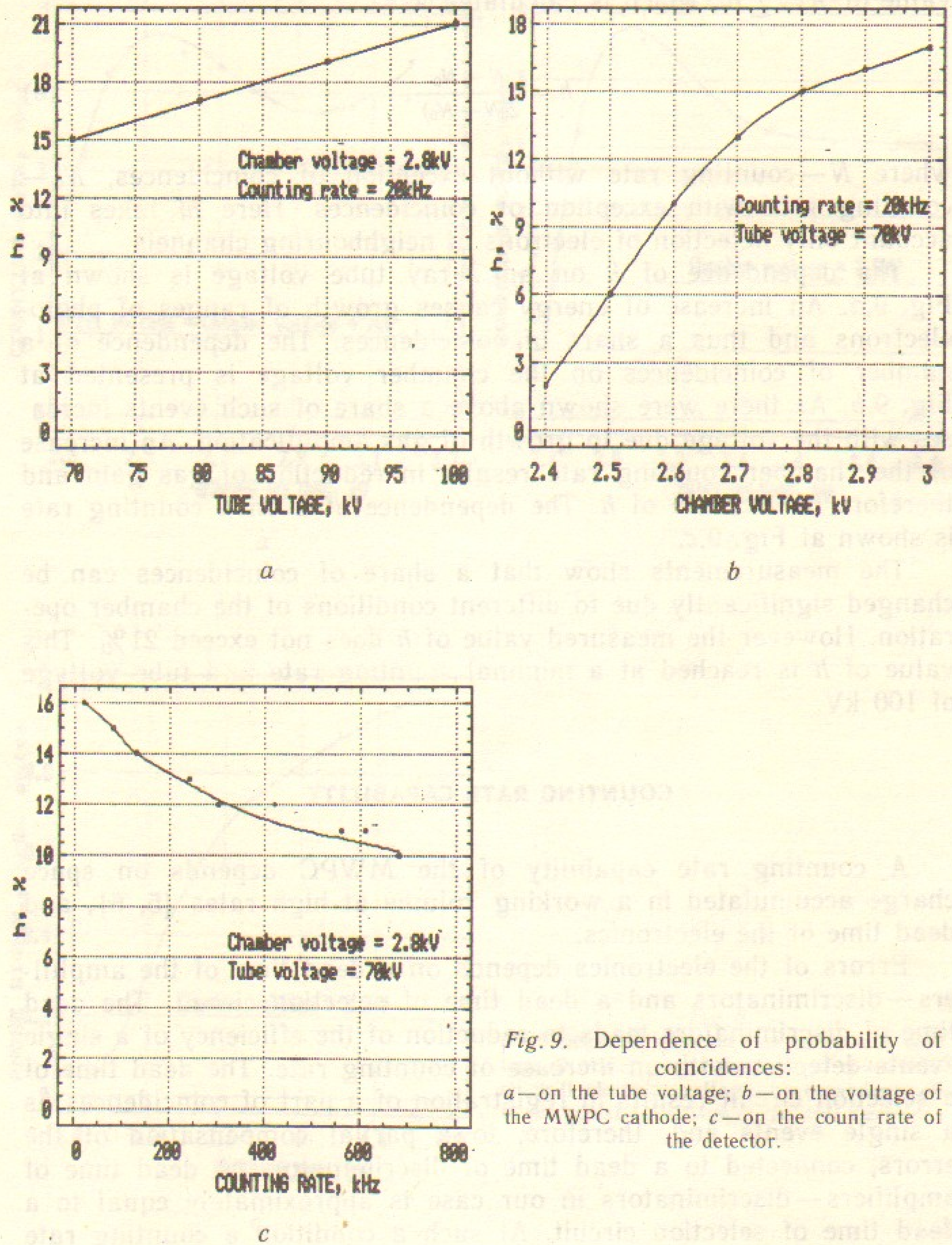

Fig. 9. Dependence of probability of coincidences:
a—on the tube voltage; *b*—on the voltage of the MWPC cathode; *c*—on the count rate of the detector.

where n_0—a frequency of single events at the input of amplifier—discriminator n_c—a frequency of coincident events; $n=n_0+n_c$—full counting rate; τ—a dead time. A selection circuit and an amplifier—discriminator have a dead time of about 200 ns. The relation between n_0 and n_c can be obtained using the expression (6) and measured value of h at a low rates: $n_c=0.43\,n_0$ (for $h=15\%$). At such a conditions the errors of electronics calculated from (7) equals 36% at the count rate of 500 kHz per channel.

The irradiation of the chamber by a uniform *X*-ray beam results in filling of the chamber volume with positive ions decreasing the electric field near the anode wires and, as a result, reducing the gas gain. The reduction of gas amplification causes the decrease of the chamber efficiency with the growth of counting rate.

The decrease of electric field is convenient to describe by a reduction of an efficient chamber voltage δV. In [6] this value was obtained for a chamber with an arbitrary geometry

$$\delta V = n_1 q \frac{l^2}{2\mu V_0 C}, \qquad (8)$$

where n_1—a counting rate per unit of length of an anode wire; q—a full charge formed in the chamber after absorbing one *X*-ray quantum; V_0—the chamber voltage; C—a capacity of a unit length of an anode wire; l—the gap between anode and cathode; μ—mobility of positive ions.

One can see from (8) that the anode—cathode gap most essentially influences the rate capability. This distance defines a thickness of space charge which reduces the field of the anode wires. That was the reason to choose the gap of 2 mm in our chamber.

The dependences of the efficiency of the MWPC on the incident flux are presented at Fig. 10. The results of measurements are shown for the chambers with anode—cathode gap of 2, 3 and 4 mm. We will call by the rate capability the counting rate at which the efficiency of the chamber decreases by 20%. The rate capability of the chambers with the gaps of 2, 3 and 4 mm equals correspondingly 600, 450 and 230 kHz/ch.

The reduction of the chamber gap l from 3 to 2 mm causes the increase of counting rate capability less than after the reduction of l from 4 to 3 mm. It is connected obviously to the fact that with gaps $l=3$ mm and less the main inefficiency is caused by electronics but not a space charge.

The main characteristic of the counting rate capability of the chamber and registration electronics, measured at a working chamber voltage and X-ray energy (Fig. 10, curve 1), shows that the

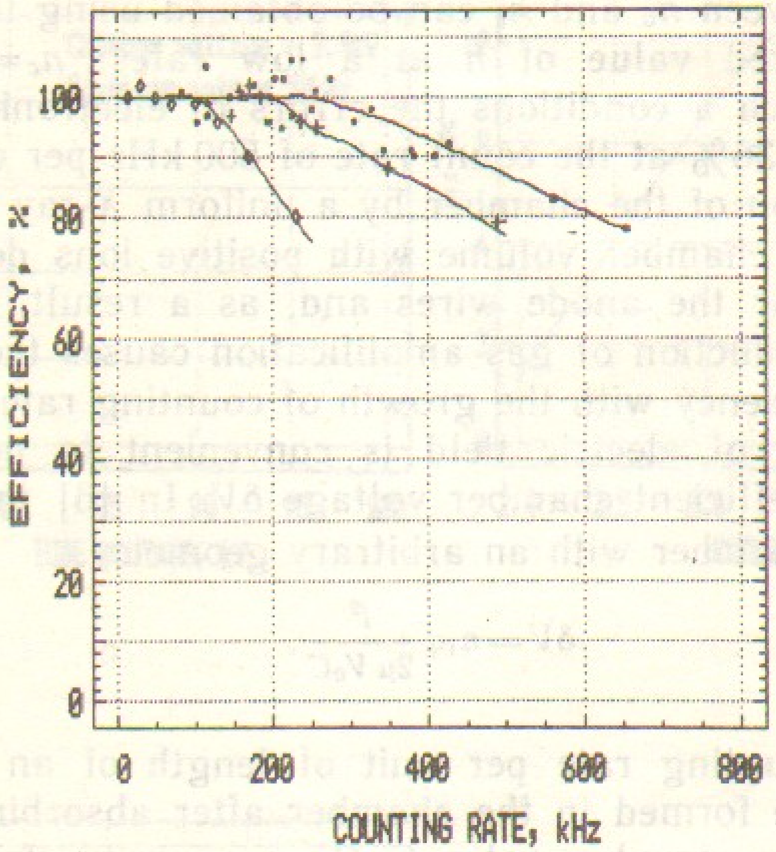

Fig. 10. Dependence of the detector efficiency on count rate:
1 — the gap between anode and cathode (l) — 2 mm; 2 — $l=3$ mm; 3 — $l=4$ mm.

rate capability obtained is higher than it follows from the expression (7), obtained only due to the dead time of the electronics. This result can be explaned taking into account the decrease of gas amplification with growth of space charge due to the increase of the counting rate, and therefore a part of coincidences, which at low n were excluded by the selection scheme now would be registrated as a single events (they exceeded a threshold of registration only in one of two neighbouring channels). Such a compensation of a loss of single events counting rate due to registration of a part of coincidences permits to obtain the detector rate capability of 600 kHz.

For a practical usage of the detector in medical diagnostics it is useful to know the dependence of the counting rate capability on the chamber voltage and the tube voltage. The results presented at Fig. 11. and 12 show that the dependence of the counting rate capability on these parameters is not very strong, that makes the chamber work stable enough.

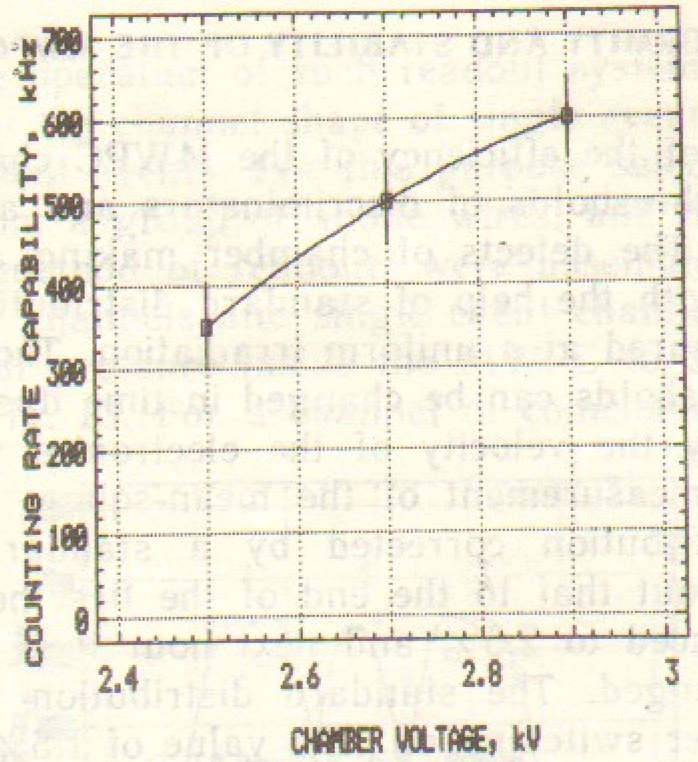

Fig. 11. Dependence of count rate capability on the voltage of MWPC.

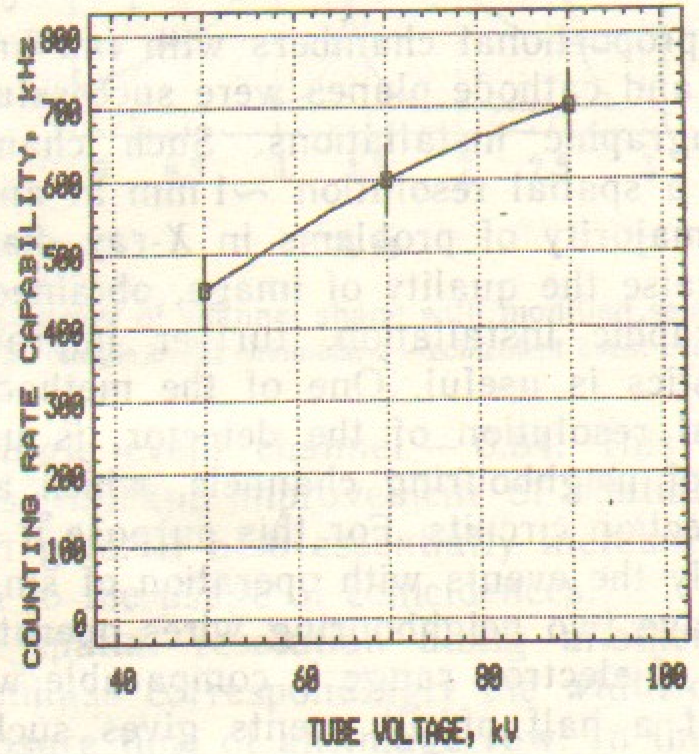

Fig. 12. Dependence of count rate capability on the voltage of X-ray tube.

UNIFORMITY AND STABILITY OF THE MWPC

Nonuniformity of the efficiency of the MWPC channels depends on differences of thresholds of discriminators and accuracy of the anode wires step. The defects of chamber making are stable and can be corrected with the help of standard distribution of chamber counting rate measured at a uniform irradiation. The differences of the electronics thresholds can be changed in time due to the system warming. To study the velocity of the electronics warming there was performed a measurement of the mean-square deviation σ of counting rate distribution corrected by a standard distribution. There were found out that to the end of the first hour after switching on σ is reduced to 2.5% and next hour it is reached 1.5%, than it is not changed. The standard distribution was measured after a 6 hours after switching on. The value of 1.5% is defined by a statistic deviation.

FUTURE DEVELOPMENT

The multiwire proportional chambers with fan anode plane and nonparallel anode and cathode planes were successfully used in the first digital radiographic installations. Such chambers give an opportunity to get a spatial resolution ~1 mm at an object, that is sufficient for the majority of problems in *X*-ray diagnostics. However, in order to raise the quality of image, obtained with the help of digital radiographic installation, further improvement of the MWPC characteristics is useful. One of the methods, allowing to improve the spatial resolution of the detector, is usage of events with coincidences of neighbouring channels, which at present time are rejected by selection circuits. For this purpose it is necessary to registrate separately the events with operation of single anode wire and those which have two neighbouring wires operated simultaneously. As the value of electron range is comparable with the step of anode wires, about a half of all events gives such coincidences. Geometrically, *X*-ray quanta, absorbed in the region between anode wires, cause coincidences, quanta, absorbed near an anode wire registrated as single events.

Such method of readout increases full value of registrated quanta approximately by a factor of two and makes the spatial resolution better.

To check the operation of such readout system there were made measurements of the channel shape of single events and the channel shape of coincident events. For this purpose selection circuits were disconnected from a group of anode wires, and the circuit, simulating described method of readout, were assembled. Efficiencies of coincident event channels and single event channels were equalized by a decrease of pressure inside the MWPC to 2 atm. The results are shown at Fig. 13. For a channel of coincidences the FWHM is

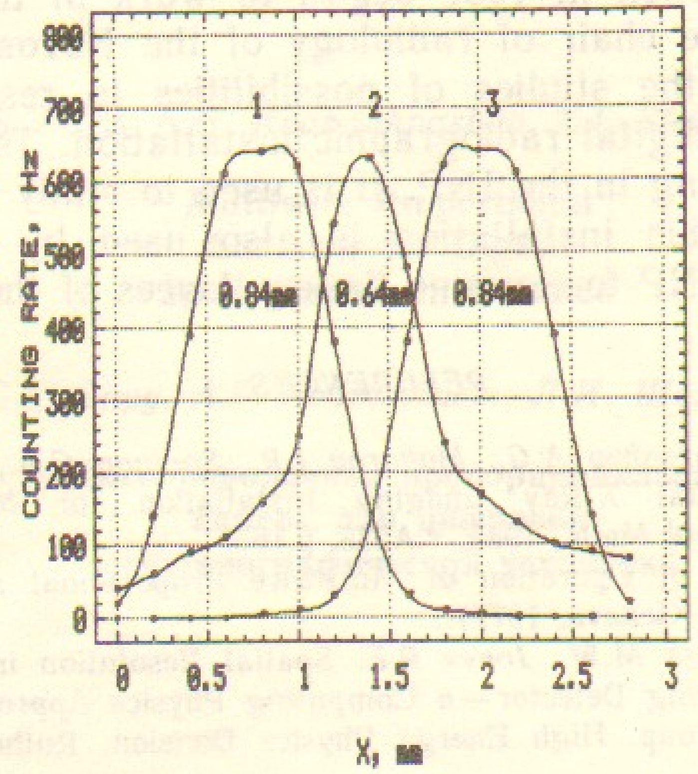

Fig. 13. The curves of channel shape with modified selection circuits: *1, 3* — single event channels; *2* — coincident event channel.

0.64 mm, for single event channel — 0.84. This result confirms a supposition of significant improvement of spatial resolution which this method can give. It also essentially increases the efficiency of the detector due to the usage of coincidences.

To improve spatial resolution along another coordinate it is necessary to diminish correspondingly the width of the slit collimator and an exposure time of an image row. In this case the number of pixels will be increased by a factor of four. Element size will be diminished to 0.5×0.5 mm (at an object).

CONCLUSIONS

Since 1984 there were made 3 radiographic installations with the MWPC described in the present paper. The first installation works from 1984 in Moscow at the All-Union Center of mother and child health protection, where it is used for study of pregnant women at a low doses (90 — 120 mR). It should be noticed for comparison that with a standard methods an exposure dose is about 2 — 3 R. The second installation in 1987 began to work in the Novosibirsk region hospital. The chair of radiology of the Novosibirsk medical institute performs the studies of possibilities to research a chest with the help of a digital radiographic installation. The third installation is now working in the INP. It is used to study characteristics of new MWPC. This installation is also used by the polyclinic department of the INP to examine the employees of the institute.

REFERENCES

1. *Baru S.E., Khabakhpashev A.G., Makarov I.R., Savinov G.A., Shekhtman L.I., Sidorov V.A.* Digital X-Ray Imaging Installation for Medical Diagnostics. — Nucl. Instr. and Meth., 1985, v.A238, p.165.
2. *Sauli F.* Principles of Operation of Multiwire Proportional and Drift Chambers. — CERN 77-09 (Geneva, 1977).
3. *Bateman J.E., Waters M.W., Jones R.E.* Spatial Resolution in a Xenon Filled MWPC X-Ray Imaging Detector — a Computing Physics Approach. — RL-75-140. Detector Physics Group. High Energy Physics Division. Rutherford laboratory (1975).
4. *Blinov N.N., Jukov E.M., Koslovsky E.B., Mazurov A.I.* Television Methods of Treatment of X-Ray and Gamma-Images. — Moscow: Energoizdat, 1982.
5. *Hendricks R.W.* Space Charge Effects in Proportional Counters. — Rev. Sci. Instr., 1969, v.40. № 9, p.1216.
6. *Mathieson E.* Dependence of Gain on Count Rate, Due to Space Charge in Co-axial and Multiwire Proportional Chambers. — Nucl. Instr. and Meth., 1986, v.A249, p.413.

S.E. Baru, A.G. Khabakhpashev, L.I. Shekhtman

Multiwire Proportional Chamber for Digital Radiographic Installation

С.Е. Бару, А.Г. Хабахпашев, Л.И. Шехтман

Многопроволочная пропорциональная камера для цифровой рентгенографической установки

Ответственный за выпуск С.Г.Попов

Работа поступила 20 января 1989 г.
Подписано в печать 23.03.89 г. МН 12025
Формат бумаги 60×90 1/16 Усл. 2,2 печ.л., 1,8 уч.-изд.л.
Тираж 290 экз. Бесплатно. Заказ № 40

Набрано в автоматизированной системе на базе фотонаборного автомата ФА1000 и ЭВМ «Электроника» и отпечатано на ротапринте Института ядерной физики СО АН СССР,
Новосибирск, 630090, пр. академика Лаврентьева, 11.